Journal of Nuclear Medicine, published on June 21, 2019 as doi:10.2967/jnumed.119.229575

# Pulmonary lymphangitic carcinomatosis: diagnostic performance of HRCT and $^{18}$F-FDG-PET/CT in correlation to clinical pathologic outcome.

**Authors:** Mario Jreige[1*], Vincent Dunet[2*], Igor Letovanec[3], John O. Prior[1], Reto A. Meuli[2], Catherine Beigelman-Aubry [2], Niklaus Schaefer[1]

* Both authors contributed equally to this work.

**Affiliation:**

[1]Department of Nuclear Medicine and Molecular Imaging, Lausanne University Hospital, Lausanne, Switzerland

[2]Department of Diagnostic and Interventional Radiology, Lausanne University Hospital, Lausanne, Switzerland

[3]Institute of Pathology, Lausanne University Hospital, Lausanne, Switzerland

**Corresponding author:**

Catherine Beigelman-Aubry, MD

Department of Diagnostic and Interventional Radiology

Lausanne University Hospital, Rue du Bugnon 46, CH-1011 Lausanne, Switzerland

E-mail: catherine.beigelman-aubry@chuv.ch

Telephone number: +41 79 556 71 54

**First authors:**

Mario Jreige, MD (resident)

Department of Nuclear Medicine and Molecular Imaging

Lausanne University Hospital, Rue du Bugnon 46, CH-1011 Lausanne, Switzerland

E-mail: mario.jreige@chuv.ch

Telephone number: +41 79 556 24 21

Vincent Dunet, MD (associated physician)

Department of Diagnostic and Interventional Radiology

Lausanne University Hospital, Rue du Bugnon 46, CH-1011 Lausanne, Switzerland

E-mail: vincent.dunet@chuv.ch

Telephone number: +41 79 556 15 38

**Running title:** PLC diagnosis on HRCT and $^{18}$F-FDG-PET/CT

**Word count:** 4’910

**ABSTRACT**

*Rationale:* To investigate the performance of high-resolution computed tomography (HRCT) versus $^{18}$F-FDG-PET/CT for the diagnosis of pulmonary lymphangitic carcinomatosis (PLC).

*Methods*: In this retrospective institutional approved study, ninety-four patients addressed for initial staging of lung cancer with suspicion of PLC were included. Using double blind analysis, we assessed the presence of signs favoring PLC on HRCT (smooth or nodular septal lines, subpleural nodularity, peribronchovascular thickening, satellite nodules, lymph node enlargement and pleural effusion). $^{18}$F-FDG-PET/CT images were reviewed to qualitatively evaluate peritumoral uptake and to quantify tracer uptake in the tumoral and peritumoral areas. Histology performed on surgical specimens served as gold standard in all patients.

*Results*: Among 94 included patients, 73% (69/94) had histologically confirmed PLC. Peribronchovascular thickening, lymph nodes involvement and increased peritumoral uptake were more often present in patients with PLC ($p<0.009$). Metabolic variables including tumor SUVmax, SUVmean, “metabolic tumor volume” (MTV) and total lesion glycolysis (TLG) as well as peritumoral SUVmax, SUVmean and their respective ratios to background were significantly higher in PLC group versus the non-PLC group ($p\leq0.0039$). Sensitivity, specificity, and ROC area [95%CI] of peribronchovascular thickening (69%, 83% and 0.76 [0.67–0.85]) and increased peritumoral uptake (94%, 84% and 0.89 [0.81–0.97]) were similar ($p=0.054$). Peritumoral SUVmax and SUVmean had a significantly higher sensitivity, specificity, and ROC area of 97%, 92% and 0.98 [0.96–1.00] and 94%, 88% and 0.96 [0.92–1.00] for detecting PLC (all $p\leq0.025$).

*Conclusion*: Qualitative evaluation of $^{18}$F-FDG-PET/CT and HRCT have similar performance for the diagnosis of PLC, both being outperformed by $^{18}$F-FDG-PET/CT quantitative parameters.

**Keywords**: Pulmonary lymphangitic carcinomatosis, lung cancer, PET/CT, FDG, HRCT.

## INTRODUCTION

Pulmonary lymphangitic carcinomatosis (PLC) was first described by Troisier in 1873 and is morphologically defined by the presence of malignant cells within pulmonary vessels, in particular the lymphatics. (*1*) Mainly originating from adenocarcinoma of the breast, stomach, lung, pancreas, and prostate, PLC may appear as bilateral symmetric pattern in case of hematogenous spread through the pulmonary arteries and subsequently into the perivascular interstitium and lymphatic vessels or as an asymmetric localized pattern with direct extension from primary lung tumor, hilar lymph nodes or pleura. (*2*) Even though definitive diagnosis of PLC requires lung biopsy, high resolution computed tomography (HRCT) is considered as an essential tool in the diagnostic process and is recommended to be performed prior to pathologic examination. (*3-5*) The few studies that investigated the role of $^{18}$F-fluorodeoxyglucose positron emission tomography ($^{18}$F-FDG-PET/CT) in the diagnosis of PLC, suggest an effective and reliable role of PET/CT as a non-invasive technique allowing PLC identification with high specificity. (*6-8*) Regarding the diagnostic performance of $^{18}$F-FDG-PET/CT, data still remain spare compared to HRCT, and no study formally evaluated the diagnostic value of quantitative PET/CT metrics compared to HRCT and PET/CT qualitative evaluations. We hence hypothetized that measure of $^{18}$F-FDG uptake in the peritumoral lung may help to detect PLC in patients with primary lung cancer.

The aim of this study was thus to investigate the diagnostic performance of HRCT versus $^{18}$F-FDG-PET/CT for the diagnosis of PLC secondary to lung cancer using the histologic gold standard, as well as to evaluate the added value of quantitative $^{18}$F-FDG-PET/CT metrics.

## MATERIALS AND METHODS

*Study Design*

The study was conducted according to Standards for Reporting of Diagnostic Accuracy Studies 2015 guidelines. (*9*) All patients referred to our Institutional Thoracic Cancer Board from December 2012 to May 2016 after initial staging of untreated lung cancer were retrospectively reviewed. Inclusion criteria were as follows: 1) patients who had both HRCT and $^{18}$F-FDG-PET/CT for initial staging within 10 weeks, 2) patients who underwent surgical resection (i.e segmentectomy, lobectomy or pneumectomy) without neoadjuvant chemotherapy. Exclusion criteria were as follows: 1) patients who underwent HRCT and $^{18}$F-FDG-PET/CT with a delay longer than 10 weeks, 2) $^{18}$F-FDG-PET/CT not performed in our institution, 3) patients who underwent neoadjuvant chemotherapy (Fig. 1). PLC, as defined by the presence of secondary invasive cells within the vessels in the peritumoral area, was ascertained on pathology reports that were used as our gold standard. For all included patients, the presence of imaging signs of PLC was evaluated on HRCT and $^{18}$F-FDG-PET/CT based on a double blinded study and correlated to clinical pathology, with less than 10 weeks (median delay: 3.5 weeks, range 0.1-10 weeks) intervening between the two modalities. The local Ethics Research Committee of the State of Vaud approved the research protocol (CER-VD #2016-01295) and, considering the retrospective nature of this study, waived the need for obtaining patient informed consent.

*$^{18}$F-FDG-PET/CT Acquisition and Analysis*

Patients underwent $^{18}$F-FDG-PET/CT on a Discovery D690 TOF (GE Healthcare,

Milwaukee, WI) 50–70 minutes after a planned intravenous injection of 3.7±0.5 MBq/kg of $^{18}$F-FDG. All patients fasted for at least 6 hours and had blood glucose levels lower than 140 mg/dl before administration of $^{18}$F-FDG. A low-dose helical CT (tube voltage: 120–140kV, tube current: 80–200mA automodulation, pitch 1.375, 0.8 sec/rotation, 3.75-mm slice thickness) was first performed for anatomical correlation and attenuation correction. Raw data were reconstructed using a blend of 40% of adaptive statistical iterative reconstruction and 60% of filtered-back-projection (FBP). Then, whole-body emission images were acquired using 7–9 overlapping bed positions of 2 min each (starting from the top of skull and ending at the mid-thigh). Images were reconstructed using ordered subset expectation maximization protocol (8 subsets, 2 iterations) with body weight-normalized SUV computation.

For each patient, SUVmax (g/ml), SUVmean (g/ml), metabolic tumoral volume (MTV) ($cm^3$) and total lesion glycolysis (TLG) ($g*cm^3/ml$) of the primary lung tumor were measured using a standard 42% SUVmax threshold volume-of-interest (VOI) embedding the whole tumor. In addition, perilesional tumoral activity was visually assessed (not increased=0, increased=1 as compared to contralateral normal lung) and quantified with measurement of peritumoral SUVmax and SUVmean within a peritumoral range of 3 cm using a VOI of 3 $cm^3$ on the most active region. Normal lung background uptake, as defined by SUVmean measured in a 3 $cm^3$ VOI within the contralateral normal lung, was used to calculate peritumoral uptake ratios as followed: peritumoral SUVmax ratio = peritumoral SUVmax / contralateral normal lung SUVmean. Peritumoral SUVmax and SUVmean measures were performed twice by two nuclear physicians with 4-years and

10-years of experience, blinded for histological results, to assess inter-observer reproducibility.

*HRCT Acquisition and Analysis*

Thoracic HRCT were performed on multiple vendor multidetector CT scanners. Due to the retrospective nature of the study, CT acquisition protocols were variables for dose parameters (tube voltage: 80–120 kV, tube intensity: 80–400 mA or mA automodulation). All raw data were reconstructed by FBP using soft and lung kernel with 1-mm slice thickness.

HRCT images of the 94 included patients were analyzed by two radiologists with respectively 25 and 10 years of experience in thoracic imaging, blinded for histological results and in consensus. The presence of smooth lines (0=absent, 1=present), nodular septal lines (0=absent, 1=present), subpleural nodularity (0=absent, 1=present), peribronchovascular thickening (0=absent, 1=present), satellite nodules (0=absent, 1=present), lymph node enlargement (0=absent, 1=present), pleural effusion (0=absent, 1=present) and enlarged pulmonary veins (0=absent, 1=present) adjacent to the primary lung tumor were recorded at the patient level.

*Histological Analysis*

All surgical specimens were prospectively analyzed by a pathologist with more than 15 years of experience in thoracic pathology and retrospectively collected. The pathologist was blinded to imaging results at the time of histological analysis. Resected lung specimens were fixed in formalin for 24–48 hours. Representative samples of the tumor

were taken, embedded in paraffin, and the slides were stained with hematoxylin and eosin. PLC was defined by the presence of secondary invasive cells within the vessels in the peritumoral area. Tumor typing was performed according to the 2011 IASLC / 2015 WHO classification. (*10*)

*Statistical Analyses*

All statistical analyses were performed using STATA version 15.1 (STATA Corp., College Station, TX, USA). Sample size calculation was performed to test equality of HRCT as compared to $^{18}$F-FDG-PET/CT. On the basis of the previous study by Prakash et al. we considered an accuracy of 93% for $^{18}$F-FDG-PET/CT, and a difference of 10% between the two methods. (*6*) We calculated a sample size of 93 patients to achieve an 80% power by using two-sided McNemar test at a significance level $\alpha$ of 0.05. Continuous variables are presented as mean ± standard deviation or median (interquartile range [IQR]). Categorical variables are presented as number or percentage. Histological outcome was used as gold standard for the diagnosis of PLC. All collected variables derived from the analysis of HRCT and $^{18}$F-FDG-PET/CT were then compared between patients with and without PLC using the Kruskal-Wallis test for continuous variables and Fisher exact test for categorical variables. Inter-observer reproducibility of peritumoral SUVmax and SUVmean was assessed by the Pearson's correlation coefficient ($\rho$) and the Lin's concordance correlation coefficient ($\rho_c = \rho \times C_b$, $C_b$ measuring systematic bias). (*11*) The association between imaging variables and PLC was assessed using logistic regression analysis with computation of respective odds ratios (OR) and 95% confidence intervals (95%CI). Odds ratios of significant predictors were compared using the Hausman's

specification test. Receiver operating characteristics (ROC) curve analysis was also performed with computation of ROC area, sensitivity, specificity, positive and negative likelihood ratio and respective 95%CI for each variable. For continuous variables, optimal cut-off values allowing detection of patients with PLC were determined by the Liu method. (*12*) ROC areas comparison was done for HRCT and $^{18}$F-FDG-PET/CT variables that were significantly associated to PLC on univariate logistic regression analysis (i.e. peribronchovascular thickening, increased peritumoral uptake and peritumoral SUVmax and SUVmean) using the non-parametric Chi-squared test of equality of ROC curves' areas, as defined by DeLong et al. (*13*) For this, we used multiple imaging parameters on univariate analysis, the significance level was corrected by the Bonferroni method to account for multiple testing. *P* values <0.003 were considered as statistically significant.

## RESULTS

### *Study Population*

Overall, 94 patients (67 males, 27 females, median age 68 years, range 44-87 years) were retrospectively included (Table 1). All underwent surgical resection and histological analysis of surgical specimens 5.9 weeks (range 0.6-22.8 months) after initial imaging evaluation. Of the 94 patients, 29 patients had stage 1 disease, 29 patients had stage 2 disease, 34 patients had stage 3 disease and 2 patients had stage 4 disease according to the 8$^{th}$ edition of the TNM classification for lung cancer. (*14*) Six patients underwent a pneumonectomy, 81 patients a lobectomy and 7 patients a segmentectomy. Fifty-five patients had adenocarcinoma, 34 patients had squamous cell carcinoma and 5 patients had poorly differentiated non-small cell carcinoma. Histological analysis additionally

confirmed PLC in 69/94 patients (73%).

*Qualitative HRCT and $^{18}$F-FDG-PET/CT Analyses*

All HRCT results are displayed in Table 1. There was no missing data for both imaging methods. Only peribronchovascular thickening (Fig. 2) was significantly correlated with the presence of PLC (OR=10.95, 95%CI:3.33–36.0, p<0.001, Table 2) and showed a ROC area, sensitivity, specificity, positive and negative likelihood ratios of 0.76 [95%CI:0.67–0.85], 69%, 83%, 4.12 and 0.38. The presence of increased peritumoral uptake in comparison to lung background had similar performance to peribronchovascular thickening with a ROC area, sensitivity and specificity of 0.89 [95%CI:0.81–0.97], 94% and 84% (p=0.054, Table 3).

Quantitative $^{18}$F-FDG-PET/CT Analysis

The inter-observer reproducibility of peritumoral SUVmax ($\rho$=0.922, $\rho_c$=0.921, $C_b$=1.0) and SUVmean ($\rho$=0.850, $\rho_c$=0.850, $C_b$=1.0) measurement was excellent. Metabolic variables including tumor TLG as well as peritumoral SUVmax, SUVmean and their respective ratios to background were significantly higher in patients with PLC compared to patients without PLC on surgical specimens (p=0.0006, p=0.0001, p=0.0001, p=0.0001 and p=0.0001, respectively, Table 1). Peritumoral SUVmax and SUVmean but not tumoral quantitative parameters were highly associated with PLC (Fig.3 and Table 3). Peritumoral SUVmax and SUVmean OR were significantly higher than OR of qualitatively increased peritumoral uptake (p=0.0022 and p=0.0005) and than OR of peribronchovascular thickening (p=0.0004 and p<0.0001). Peritumoral SUVmax with a

cut-off of 2.1 g/ml had a significantly higher sensitivity, specificity, and ROC area of 97%, 92% and 0.98 [95%CI:0.96-1.00] for detecting PLC compared to both qualitatively increased peritumoral uptake (p=0.0064) and peribronchovascular thickening (p<0.0001, Fig. 4). Peritumoral SUVmean with a cut-off of 1.2 g/ml also had higher performance for detecting PLC compared to increased peritumoral uptake (p=0.025) and peribronchovascular thickening (p<0.0001). The diagnostic performance of absolute peritumoral SUVmax, peritumoral SUVmean, peritumoral SUVmax ratio and peritumoral SUVmean ratio were similar (p≥0.10).

## DISCUSSION

In this study, we showed that $^{18}$F-FDG-PET/CT and HRCT had similar performance for the diagnosis of PLC in patients addressed for initial staging of primary lung tumor when respectively qualitatively evaluating increased peritumoral uptake and peribronchovascular thickening. Other signs such as smooth or nodular septal lines, subpleural nodularity, satellite nodules, or pleural effusion were not significantly associated with PLC. Moreover, $^{18}$F-FDG uptake quantification in the peritumoral area outperformed qualitative analysis of both modalities.

The pathogenesis of pulmonary tumor embolism and lymphangitic carcinomatosis is poorly understood. It is thought that in PLC tumor cells gain access to the lung vascular system – and particularly to the lymphatic system – to induce local tumoral spread via neovasculature or neolymphatics in case of lung primary. In the case of non-pulmonary primary tumors, the cells spread via retrograde flow since the majority of these malignancies involve thoracic lymph nodes. Invasion of the interstitial space by tumor

cells or in distended lymphatic vessels can result in thickened peribronchovascular bundles and septa. (*15-17*) Tumor cells trapped within lymphatics result in local obstruction and fluid accumulation. Thus, peribronchovascular bundle and alveolar septal thickening may be due to local edema. (*1*) Any malignant tumor has the potential to result in pulmonary tumor embolism, whether as PLC or as pulmonary tumor emboli, with higher incidence in patients with renal cell and hepatocellular carcinoma as well as adenocarcinoma of the breast, stomach, colon, and lung. (*18, 19*) This pattern of tumor spread is not common and occurs in less than 10% of metastatic cancers in the lung. (*2*) The definitive diagnosis of PLC depends upon the identification of tumor cells in the pulmonary lymphatics on histological examination, which allows identifying obstruction and distension of pleural, peribronchial, perivascular or subpleural lymphatics. (*17*) PLC is typically an advanced-stage manifestation of malignancy and is associated with poor prognosis. (*20-22*).

Common findings associated with PLC on HRCT include thickening of interlobular septa and peribronchovascular interstitium, sub-pleural nodules, thickening of the interlobar fissures, pleural effusion, pleural carcinomatosis, hilar and mediastinal nodal enlargement with relatively little destruction of overall lung architecture. (*4*) However, smooth or thickened interlobular septa on HRCT, in particular with nodular appearance are not being specific for PLC since it is also encountered in other interstitial disorders such as sarcoidosis (*23*) Hilar adenopathy and effusions were occasionally present in reported series of PLC. (*24*)

In a retrospective study on 21 patients, when correlated to pathology, certain characteristic findings on CT scans were evident: uneven thickening of

peribronchovascular bundles, thickening of isolated interstitial lines, and the presence of polygonal lines. The pathologic basis for these characteristic CT findings was considered by the authors as related to tumor thrombi in lymphatic vessels rather than edema and fibrosis, at least in the early stages of disease. (*25*) Another study reported that thickening of peribronchovascular bundles and interlobular septa is the single most important chest CT finding of pulmonary lymphangitic carcinomatosis. (*26*) Our study hereby confirms that peribronchovascular thickening and lymph node enlargement should mainly be considered as signs of PLC at initial staging, while first reporting diagnostic performance parameters of HRCT in this setting.

Regarding $^{18}$F-FDG-PET/CT, we described the largest series of patients with histologically proven PLC and who underwent imaging with a state-of-the art $^{18}$F-FDG-PET/CT scanner. To the best of our knowledge, only three studies reported on the role of $^{18}$F-FDG-PET/CT in the diagnosis of PLC. In a retrospective study of 35 patients, Prakash et al. found a high specificity of 100% of $^{18}$F-FDG-PET/CT in the detection of PLC with a sensitivity of 86%. (*6*) In addition, this study reported a statistically significant increased $^{18}$F-FDG uptake in the PLC areas in contrast to normal lung parenchyma and blood pool activity, in concordance with our results. In a group of 7 patients with PLC, Digumarthy et al. reported that the intensity of $^{18}$F-FDG uptake in diseased lung is significantly greater than in corresponding normal contralateral lung or in the lungs of normal controls with a ratio of the SUV of lung with lymphangitic carcinomatosis to corresponding contralateral normal lung significantly increased. (*8*) In a series of five PLC positive cases, Acikgoz et al. described the $^{18}$F-FDG-PET/CT pattern, varying from a diffuse, lobar, or segmental $^{18}$F-FDG uptake in the lungs in extensive PLC to a hazy area of $^{18}$F-FDG uptake or linear

uptake extending from the tumor to the lymph nodes in limited PLC. The route of lymphangitic spread in these cases was considered either through seeding of tumor cells to the peribronchovascular lymphatics or direct invasion of lymphatics by the lung tumor. (*7*) While we confirm that increased peritumoral uptake may be useful for the detection of PLC, its performance is not superior to peribronchovascular thickening on HRCT. Moreover, we first demonstrate that adding peritumoral SUV and ratio to lung background measurement significantly improve the performance of $^{18}$F-FDG-PET/CT for the diagnosis of PLC. Quantitative $^{18}$F-FDG-PET/CT of peritumoral areas should hence be part of the initial imaging workup of patients with primary lung cancer. It is however worthy to mention that CT images should always be checked before measuring peritumoral SUV in order to avoid misinterpretation of peritumoral infiltrates from another etiology such as infection (*27*). In the area of hybrid imaging, acquisition of HRCT images during a single contrast enhanced $^{18}$F-FDG–PET/HRCT examination should be the next step to optimize patients' evaluation and minimize costs. This has to be evaluated further.

We have to address some limitations of our study. First, due to its retrospective nature, HRCT images were acquired on multiple vendor CT scanners with variable acquisition parameters but similar reconstruction parameters. Although image quality may be different, it reflects daily practice of our thoracic oncology board. Second, HRCT images were assessed by experts in thoracic imaging. While qualitative evaluation of HRCT and $^{18}$F-FDG-PET/CT demonstrated similar performance, the learning curve to detect subtle peribronchovascular thickening on HRCT may be an issue to reproduce this result in daily practice, especially in situations such as COPD patients with bronchial wall thickening. Third, only patients who underwent surgical resection were included. While this allowed

histological confirmation of PLC, reported cut-off values of quantitative metrics may not be fully transposable in inoperable patients, as it may not be transposable using different PET scanner or reconstruction algorythm. However, use of peritumoral SUV ratios may overwhelm this limitation, with similar diagnostic confidence. Finally, while the use of $^{18}$F-FDG-PET/CT quantitative parameters improved the diagnostic performance of $^{18}$F-FDG-PET/CT for PLC, the prognostic value of these metrics at initial staging remains unknown. This was out of the scope of the present study and should be further assessed to fully evaluate the usefulness of these measurements.

## CONCLUSION

Our study showed that peribronchovascular thickening and increased peritumoral tracer uptake, respectively on HRCT and $^{18}$F-FDG-PET/CT, have similar performance for the diagnosis of PLC in patients with lung cancer at initial staging. Peritumoral $^{18}$F-FDG uptake quantification however outperformed qualitative evaluation. Combining resultant morphologic and metabolic criteria may thus help to establish a powerful tool for the diagnosis of PLC.

## DISCLOSURE

The authors have no potential conflict of interest to report.

**KEY POINTS**

QUESTION: To compare the performance of HRCT versus $^{18}$F-FDG-PET/CT for the diagnosis of pulmonary lymphangitic carcinomatosis (PLC).

PERTINENT FINDINGS: Peribronchovascular thickening and increased peritumoral tracer uptake, respectively on HRCT and $^{18}$F-FDG-PET/CT, have similar performance for the diagnosis of pulmonary lymphangitic carcinomatosis in patients with lung cancer at initial staging.

Peritumoral $^{18}$F-FDG uptake quantification however outperforms qualitative evaluation on both modalities.

IMPLICATIONS FOR PATIENT CARE: Combining morphologic and metabolic parameters may help establish a powerful tool for the diagnosis of pulmonary lymphangitic carcinomatosis.

## REFERENCES


1. Bruce DM, Heys SD, Eremin O. Lymphangitis carcinomatosa: a literature review. *J R Coll Surg Edinb.* 1996;41:7-13.

2. Janower ML, Blennerhassett JB. Lymphangitic spread of metastatic cancer to the lung. A radiologic-pathologic classification. *Radiology.* 1971;101:267-273.

3. Regueiro F, Roche P, Regueiro MV, Lozano R. The importance of histology in the evaluation of pulmonary transplantation: carcinomatous lymphangitis. *Thorac Cardiovasc Surg.* 2005;53:122-123.

4. Torrington KG, Hooper RG. Diagnosis of lymphangitic carcinomatosis by transbronchial lung biopsy. *South Med J.* 1978;71:1487-1488.

5. Mathieson JR, Mayo JR, Staples CA, Muller NL. Chronic diffuse infiltrative lung disease: comparison of diagnostic accuracy of CT and chest radiography. *Radiology.* 1989;171:111-116.

6. Prakash P, Kalra MK, Sharma A, Shepard JA, Digumarthy SR. FDG PET/CT in assessment of pulmonary lymphangitic carcinomatosis. *AJR Am J Roentgenol.* 2010;194:231-236.

7. Acikgoz G, Kim SM, Houseni M, Cermik TF, Intenzo CM, Alavi A. Pulmonary lymphangitic carcinomatosis (PLC): spectrum of FDG-PET findings. *Clin Nucl Med.* 2006;31:673-678.

8. Digumarthy SR, Fischman AJ, Kwek BH, Aquino SL. Fluorodeoxyglucose positron emission tomography pattern of pulmonary lymphangitic carcinomatosis. *J Comput Assist Tomogr.* 2005;29:346-349.

9. Cohen JF, Korevaar DA, Altman DG, et al. STARD 2015 guidelines for reporting diagnostic accuracy studies: explanation and elaboration. *BMJ Open.* 2016;6:e012799.

10. Gurda GT, Zhang L, Wang Y, et al. Utility of five commonly used immunohistochemical markers TTF-1, Napsin A, CK7, CK5/6 and P63 in primary and metastatic adenocarcinoma and squamous cell carcinoma of the lung: a retrospective study of 246 fine needle aspiration cases. *Clin Transl Med.* 2015;4:16.

11. Lin LI. A concordance correlation coefficient to evaluate reproducibility. *Biometrics.* 1989;45:255-268.

12. Liu X. Classification accuracy and cut point selection. *Stat Med.* 2012;31:2676-2686.

13. DeLong ER, DeLong DM, Clarke-Pearson DL. Comparing the areas under two or more correlated receiver operating characteristic curves: a nonparametric approach. *Biometrics.* 1988;44:837-845.

14. Detterbeck FC, Boffa DJ, Kim AW, Tanoue LT. The Eighth Edition Lung Cancer Stage Classification. *Chest.* 2017;151:193-203.

15. Soares FA, Pinto AP, Landell GA, de Oliveira JA. Pulmonary tumor embolism to arterial vessels and carcinomatous lymphangitis. A comparative clinicopathological study. *Arch Pathol Lab Med.* 1993;117:827-831.

16. Lindqvist C, Lepantalo M, Jungell P. Lymphangitis carcinomatosa of the lungs. An unusual complication of oral cancer. *Br J Oral Maxillofac Surg.* 1988;26:228-231.

17. Sakuma M, Fukui S, Nakamura M, et al. Cancer and pulmonary embolism: thrombotic embolism, tumor embolism, and tumor invasion into a large vein. *Circ J.* 2006;70:744-749.

18. Roberts KE, Hamele-Bena D, Saqi A, Stein CA, Cole RP. Pulmonary tumor embolism: a review of the literature. *Am J Med.* 2003;115:228-232.

19. King MB, Harmon KR. Unusual forms of pulmonary embolism. *Clin Chest Med.* 1994;15:561-580.

20. Bassiri AG, Haghighi B, Doyle RL, Berry GJ, Rizk NW. Pulmonary tumor embolism. *Am J Respir Crit Care Med.* 1997;155:2089-2095.

21. Moubax K, Wuyts W, Vandecaveye V, Prenen H. Pulmonary lymphangitic carcinomatosis as a primary manifestation of gastric carcinoma in a young adult: a case report and review of the literature. *BMC Res Notes.* 2012;5:638.

22. Gonzalez-Vitale JC, Garcia-Bunuel R. Pulmonary tumor emboli and cor pulmonale in primary carcinoma of the lung. *Cancer.* 1976;38:2105-2110.

23. Chan CK, Hutcheon MA, Hyland RH, Smith GJ, Patterson BJ, Matthay RA. Pulmonary tumor embolism: a critical review of clinical, imaging, and hemodynamic features. *J Thorac Imaging.* 1987;2:4-14.

24. Shepard JA, Moore EH, Templeton PA, McLoud TC. Pulmonary intravascular tumor emboli: dilated and beaded peripheral pulmonary arteries at CT. *Radiology.* 1993;187:797-801.

25. Munk PL, Muller NL, Miller RR, Ostrow DN. Pulmonary lymphangitic carcinomatosis: CT and pathologic findings. *Radiology.* 1988;166:705-709.

26. Johkoh T, Ikezoe J, Tomiyama N, et al. CT findings in lymphangitic carcinomatosis of the lung: correlation with histologic findings and pulmonary function tests. *AJR Am J Roentgenol.* 1992;158:1217-1222.

27. Hou S, Lin X, Wang S, et al. Combination of positron emission tomography/computed tomography and chest thin-layer high-resolution computed tomography for evaluation of pulmonary nodules: Correlation with imaging features, maximum standardized uptake value, and pathology. *Medicine (Baltimore).* 2018;97:e11640.

**FIGURES**

FIGURE 1. Study flowchart.

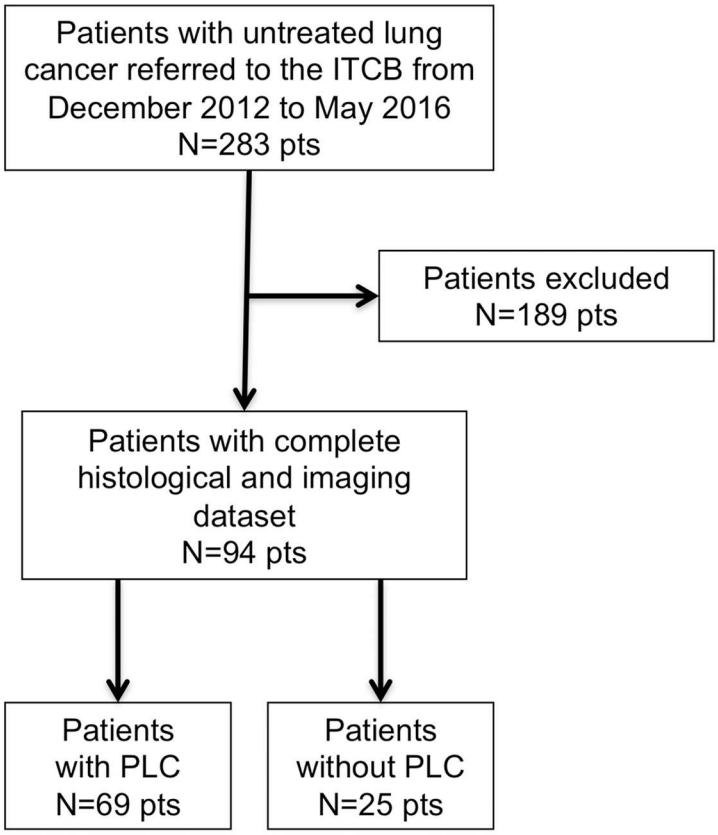


ITCB= Institutional Thoracic Cancer Board, PLC= pulmonary lymphangitic carcinomatosis

FIGURE 2. Case of a 66-year-old female referred for initial staging of inferior lobe pulmonary adenocarcinoma (Stage IIIA). HRCT (A) shows positive peribronchovascular thickening sign (yellow arrow) and $^{18}$F-FDG-PET/CT (B) shows $^{18}$F-FDG uptake in the corresponding region higher than background, with a SUVmax of 2.5 g/ml and a SUVmax to background ratio of 3.6.

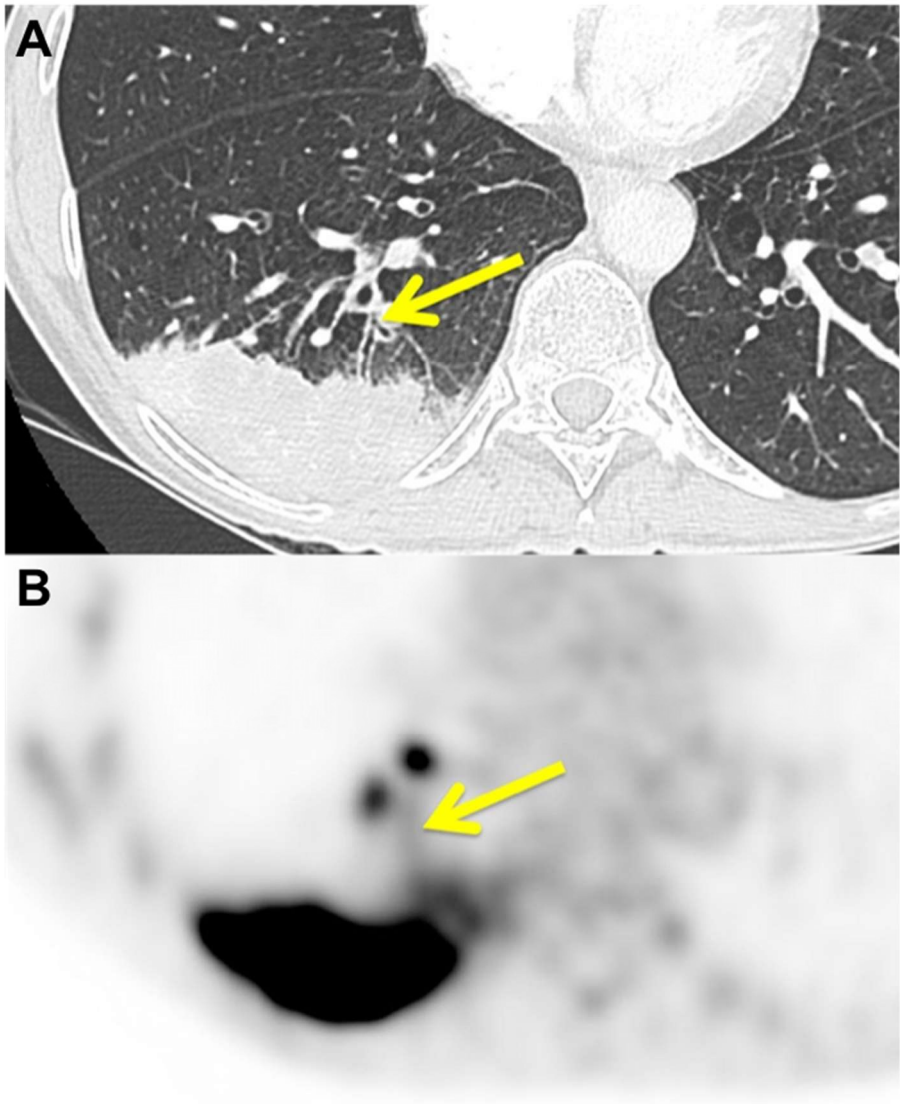

FIGURE 3. Boxplot showing a significant difference of SUVmax values in the peritumoral region on $^{18}$F-FDG-PET/CT in patients with (PLC+) and without PLC (PLC–).

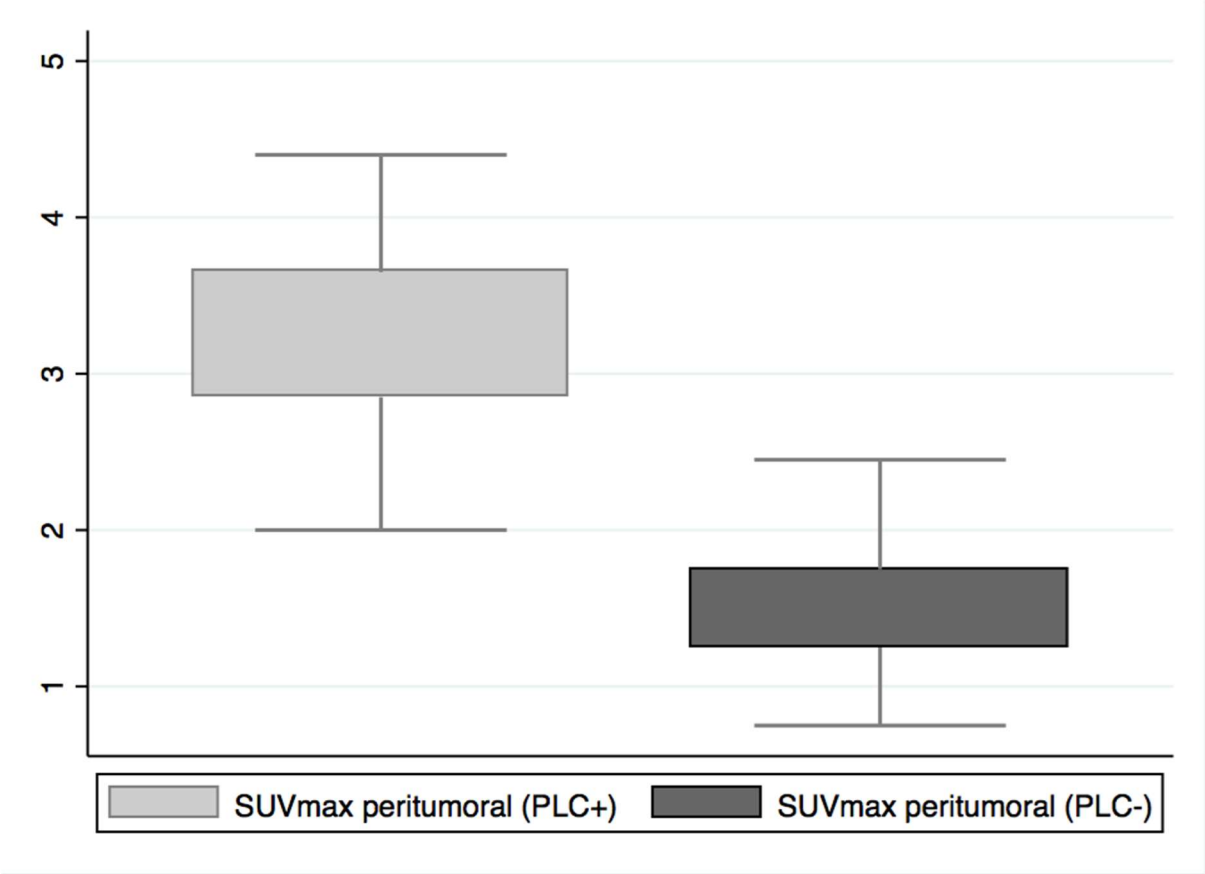

FIGURE 4. ROC curves comparing the performance of peribronchovascular thickening on HRCT (red line, ROC area=0.76 [0.67–0.85]) and SUVmax in the peritumoral region on $^{18}$F-FDG-PET/CT (navy line, ROC area=0.98 [0.96–1.00]) for the diagnosis of PLC ($p<0.0001$).

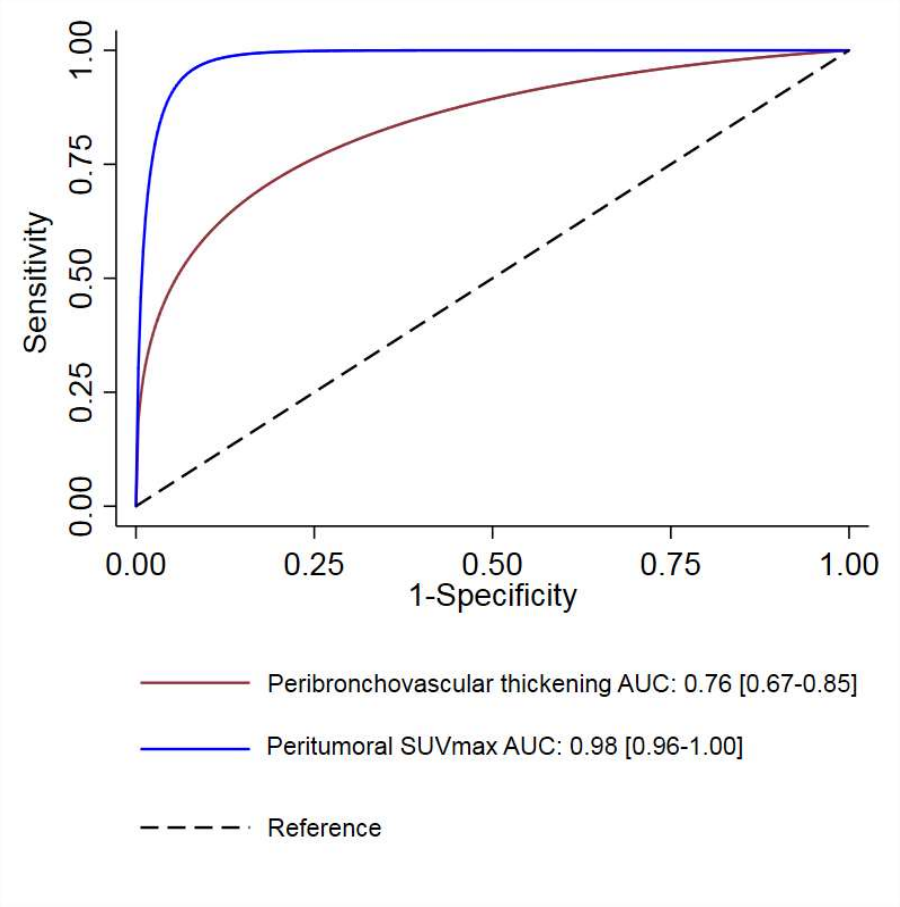

## TABLES

TABLE 1. Clinico-pathological characteristics and results of HRCT and $^{18}$F-FDG-PET/CT evaluation in patients without and with PLC.

| Variables | Without PLC n=25 | With PLC n=69 | p-value |
|---|---|---|---|
| ***Characteristics*** | | | |
| Age | 67±10 | 66±9 | 0.81 |
| Gender (male/female) | 18/7 | 49/20 | 0.57 |
| TNM stage<br>1<br>2<br>3<br>4 | <br>16<br>6<br>2<br>1 | <br>13<br>23<br>32<br>1 | <0.001 |
| Surgery<br>Segmentectomy<br>Lobectomy<br>Pneumonectomy | <br>3<br>22<br>0 | <br>4<br>59<br>6 | 0.21 |
| ***Histology***<br>Adenocarcinoma<br>Poorly differentiated NSCLC<br>Squamous cell carcinoma | <br>19<br>0<br>6 | <br>36<br>5<br>28 | 0.081 |
| ***HRCT*** | | | |
| Smooth lines | 19 | 60 | 0.45 |
| Nodular lines | 3 | 13 | 0.62 |
| Peribronchovascular thickening | 4 | 46 | 0.0002 |
| Subpleural space | 3 | 4 | 0.64 |
| Satellite nodes | 6 | 12 | 0.61 |
| Enlarged lymph nodes | 7 | 44 | 0.0082 |
| Pleural effusion | 3 | 9 | 0.95 |
| Enlarged pulmonary veins | 4 | 4 | 0.44 |
| ***PET Qualitative*** | | | |
| Peritumoral increased uptake | 4 | 65 | 0.0001 |
| ***PET Quantitative*** | | | |
| Tumor SUVmax (g/mL) | 9.1±7.1 | 14.1±8.0 | 0.0031 |
| Tumor SUVmean (g/mL) | 5.5±4.7 | 8.4±5.1 | 0.0039 |
| MTV ($cm^3$) | 9.6±9.4 | 22.3±23.3 | 0.0031 |
| TLG ($g.cm^3/mL$) | 72.9±119.4 | 225.8±322.7 | 0.0006 |
| Peritumoral SUVmax (g/mL) | 1.5±0.4 | 3.2±0.6 | 0.0001 |
| Peritumoral SUVmean (g/mL) | 0.9±0.3 | 1.8±0.4 | 0.0001 |
| Peritumoral SUVmax ratio (1) | 1.6±0.5 | 3.2±0.7 | 0.0001 |
| Peritumoral SUVmean ratio (1) | 1.7±0.6 | 3.1±0.9 | 0.0001 |

HRCT= high-resolution computed tomography, MTV= metabolic tumoral volume, NSCLC= non-small cell lung carcinoma, PET= positron emission tomography, PLC= pulmonary lymphangitic carcinomatosis, SUV= standardized uptake value, TLG= total lesion glycolysis, TNM=tumor node metastasis. P-values were obtained using the

Kruskal-Wallis test for continuous variables and Fisher exact test for categorical variables. For imaging parameters, P values <0.003 were considered statistically significant to account for multiple comparisons.

TABLE 2. Results of association of HRCT variables with PLC: odds ratios (OR) with 95% confidence interval, as well as ROC area, sensitivity (Se), specificity (Sp), positive and negative likelihood ratios (LR+ and LR-) with 95% confidence interval.

| HRCT variables | OR | p-value | ROC area | Se | Sp | LR+ | LR- |
|---|---|---|---|---|---|---|---|
| Smooth lines | 2.26 (0.64-7.94) | 0.21 | 0.55 (0.46-0.64) | 0.90 (0.80-0.96) | 0.21 (0.07-0.42) | 1.13 (0.91-1.41) | 0.50 (0.18-1.43) |
| Nodular lines | 1.69 (0.44-6.52) | 0.45 | 0.53 (0.45-0.62) | 0.19 (0.11-0.31) | 0.88 (0.68-0.97) | 1.55 (0.48-4.98) | 0.92 (0.76-1.12) |
| Peribronchovascular thickening | 10.95 (3.33-36.0) | <0.001 | 0.76 (0.67-0.85) | 0.69 (0.56-0.79) | 0.83 (0.63-0.95) | 4.12 (1.66-10.2) | 0.38 (0.25-0.56) |
| Subpleural space | 0.44 (0.09-2.15) | 0.31 | 0.47 (0.39-0.54) | 0.06 (0.02-0.15) | 0.88 (0.68-0.97) | 0.48 (0.12-1.98) | 1.07 (0.91-1.26) |
| Satellite nodes | 0.65 (0.21-2.00) | 0.46 | 0.46 (0.36-0.56) | 0.18 (0.10-0.29) | 0.75 (0.53-0.90) | 0.72 (0.30-1.70) | 1.09 (0.85-1.41) |
| Enlarged lymph nodes | 4.65 (1.68-12.8) | 0.003 | 0.68 (0.57-0.79) | 0.66 (0.53-0.77) | 0.71 (0.49-0.87) | 2.25 (1.18-4.3) | 0.48 (0.32-0.74) |
| Pleural effusion | 1.09 (0.27-4.40) | 0.91 | 0.50 (0.43-0.58) | 0.13 (0.06-0.24) | 0.88 (0.68-0.97) | 1.07 (0.32-3.64) | 0.99 (0.83-1.18) |
| Enlarged pulmonary veins | 0.32 (0.07-1.39) | 0.13 | 0.45 (0.37-0.53) | 0.06 (0.02-0.15) | 0.83 (0.63-0.95) | 0.36 (0.10-1.32) | 1.13 (0.93-1.36) |

HRCT= high resolution computed tomography, PLC= pulmonary lymphangitic carcinomatosis. P values <0.003 were considered statistically significant to account for multiple testing.

TABLE 3. Results of association of $^{18}$F-FDG-PET/CT variables with PLC: odds ratios (OR) with 95% confidence interval, as well as ROC area, cut-off values determined by the Liu method, sensitivity (Se), specificity (Sp), positive and negative likelihood ratios (LR+ and LR-) with 95% confidence interval.

| **$^{18}$F-FDG-PET/CT variables** | **OR** | **p-value** | **ROC area** | **Cut-off values** | **Se** | **Sp** | **LR+** | **LR-** |
|---|---|---|---|---|---|---|---|---|
| ***PET Qualitative*** | | | | | | | | |
| Peritumoral increased uptake | 85.31 (19.6-371) | <0.001 | 0.89 (0.81-0.97) | — | 0.94 (0.86-0.98) | 0.84 (0.64-0.96) | 5.89 (2.39-14.5) | 0.07 (0.03-0.18) |
| ***PET Quantitative*** | | | | | | | | |
| Tumor SUVmax (g/mL) | 1.10 (1.02-1.18) | 0.011 | 0.70 (0.58-0.83) | 9.1 | 0.74 (0.62-0.84) | 0.64 (0.43-0.82) | 2.05 (1.2-3.53) | 0.41 (0.25-0.67) |
| Tumor SUVmean (g/mL) | 1.15 (1.02-1.29) | 0.019 | 0.70 (0.57-0.82) | 5.5 | 0.73 (0.60-0.83) | 0.64 (0.43-0.82) | 2.01 (1.17-3.46) | 0.43 (0.27-0.70) |
| MTV ($cm^3$) | 1.06 (1.00-1.11) | 0.022 | 0.70 (0.58-0.82) | 11.3 | 0.55 (0.43-0.67) | 0.76 (0.55-0.91) | 2.29 (1.11-4.76) | 0.59 (0.42-0.83) |
| TLG ($g.cm^3$/mL) | 1.00 (1.00-1.01) | 0.027 | 0.73 (0.61-0.85) | 14.6 | 0.90 (0.80-0.96) | 0.52 (0.31-0.72) | 1.87 (1.24-2.84) | 0.20 (0.09-0.43) |
| Peritumoral SUVmax (g/mL) | 312. (13.7-7124) | <0.001 | 0.98 (0.96-1.00) | 2.1 | 0.97 (0.90-1.00) | 0.92 (0.74-0.99) | 12.14 (3.21-45.9) | 0.03 (0.01-0.12) |
| Peritumoral SUVmean (g/mL) | 724 (41.70-12593) | <0.001 | 0.96 (0.92-1.00) | 1.2 | 0.94 (0.86-0.98) | 0.88 (0.69-0.98) | 7.85 (2.71-22.7) | 0.07 (0.03-0.17) |
| Peritumoral SUVmax ratio (1) | 63.0 (9.89-401) | <0.001 | 0.96 (0.92-1.00) | 2.3 | 0.93 (0.84-0.98) | 0.88 (0.69-0.98) | 7.73 (2.67-22.4) | 0.08 (0.04-0.19) |
| Peritumoral SUVmean ratio (1) | 16.9 (5.24-54.5) | <0.001 | 0.92 (0.84-0.99) | 2.4 | 0.84 (0.73-0.92) | 0.92 (0.74-0.99) | 10.51 (2.77-39.9) | 0.17 (0.10-0.30) |

MTV= metabolic tumor volume, PET= positron emission tomography, PLC= pulmonary lymphangitic carcinomatosis, SUV= standardized uptake value, TLG= total lesion glycolysis, TNM=tumor node metastasis. P values <0.003 were considered statistically significant to account for multiple testing.